Supplementary Appendix

Supplement to: Vogt MR, Wright PF, Hickey WF, De Buysscher T, Boyd KL, Crowe JE Jr. Enterovirus D68 in the anterior horn cells of a child with acute flaccid myelitis. N Engl J Med 2022;386:2059-60. DOI: 10.1056/NEJMc2118155

This appendix has been provided by the authors to give readers additional information about the work.

TABLE OF CONTENTS

INTRODUCTION

The term acute flaccid myelitis (AFM) was coined in 2014 after an outbreak across the United States that affected 120 patients in the late summer and fall months[1]. Retrospective analysis, however, suggests that cases of AFM have occurred in earlier years, including a California outbreak in 2012[2]. The paralysis of AFM affects mostly skeletal muscles of the extremities, but in severe cases can progress to bulbar paralysis, affecting the muscles of swallowing and breathing[3]. In children with AFM, as long as the onset of limb paralysis is recognized before progression to bulbar paralysis, supportive care such as positive pressure ventilation and direct gastric feeding typically prevents death. Recovery from AFM is highly variable but rarely involves full recovery of all strength[4]. While AFM is a highly morbid disease, mortality is low, with only two reported deaths out of 668 confirmed AFM cases since 2014 in the United States[5].

The outbreaks of AFM disease seen in the U.S. in 2014, 2016, and 2018 all have coincided with the occurrence of enterovirus D68 (EV-D68) infections in at risk populations. Over time, evidence has grown to show a causal link between EV-D68 infection and AFM[6]. The supportive evidence of a causal link includes using murine models of infection in which EV-D68 can infect motor neurons in the anterior horn of the spinal cord, with paralysis in the corresponding innervated limbs[7,8]. Also, immune cell infiltrates predominate surrounding infected motor neurons in mice[8]. *In vitro* experiments with differentiated human induced pluripotent stem cells (iPSCs) have shown that EV-D68 infects both neuron- and astrocyte-like cells in culture[9,10].

Twelve years after his death, we returned to this patient's autopsy specimens now that we understand the significance of EV-D68 causing outbreaks of AFM to more deeply investigate the

pathology and immune response in this patient. We found that EV-D68 genomic RNA and capsid protein was present within the neurons but not the glial cells of the anterior horn of the spinal cord. Immune infiltrates of infected spinal cord were mainly composed of CD68+ macrophages and CD8+ T cells. Spatial immune transcriptome analysis showed upregulation of antigen processing pathways for class I MHC presentation.

CLINICAL CASE

The patient in this study was a five-years-old male who was putatively in good health until developing symptoms of an upper respiratory tract infection coincident with a similar illness in many of his classmates in fall of 2008. Three days into this illness, he first experienced asymmetric weakness in his upper extremities and change was noted in the timbre of his voice. This presentation gradually progressed, and by day five of illness he had difficulty walking. That night he was found in bed to be apneic and on arrival to the hospital was unable to be resuscitated. His previously reported autopsy showed the presence of a T cell infiltrate in the spinal cord with neurons that stained positive for perforin and negative for caspase. Sequencing of RNA from his cerebrospinal fluid by the Centers for Disease Control and Prevention identified EV-D68 viral RNA[11].

METHODS

We searched the medical literature for all available years in PubMed (https://pubmed.ncbi.nlm.nih.gov) on June 20, 2020 for reports of cases of patients who died during the acute illness of AFM. This patient was the only identified from whom we obtained specimens[11], although at least two other deaths had been noted in Europe[12]. We used

formaldehyde fixed and paraffin embedded (FFPE) tissues from the 2008 autopsy in all studies described below.

IMMUNOHISTOCHEMISTRY

Slides were deparaffinized, then heat-induced antigen retrieval was performed using Leica Epitope Retrieval 2 solution for 20 min for all staining except NeuN, that used Epitope Retrieval 1 solution. Slides were incubated with antibody for 15 min to 1 hr. The Bond Polymer Refine detection system was used for visualization. Slides were dehydrated, cleared and coverslipped. All steps besides dehydration, clearing and coverslipping were performed on the Leica Bond Max IHC stainer. The antibodies used stained the following antigens: EV-D68 VP2 capsid protein (GeneTex #132312), CD68 (StatLab #MM36-10), CD20 (StatLab #MM07-10), CD8 (StatLab #MM39-10), CD4 (Leica #PA0427), CD3 (StatLab #MM150-10), and NeuN (Millipore/Sigma #MAB377).

IN SITU HYBRIDIZATION

The EV-D68 VP1 gene sequence generated from the cerebrospinal fluid that was originally used to identify EV-D68 (GenBank accession #MT106051) was used as template to generate oligonucleotide target probes for *in situ* hybridization of spinal cord tissue (BaseScope kit; Advanced Cell Diagnostics, Inc.).

As a positive control for both the immunohistochemistry and the *in situ* hybridization, we used human origin cell lines (RD cells, ATCC #CCL-136) that were experimentally infected with EV-D68 *in vitro* and then fixed and paraffin embedded. For negative controls, we used uninfected RD cells, and from human specimens we included normal tonsil and placenta, and

from this specimen we used neurons in the unaffected regions in the same tissue section (contralateral region and posterior region of the spinal cord).

SPATIAL IMMUNOMICS

Sections of spinal cord tissue were tested for the location and quantification of human gene transcripts and gene products in tissue with a commercial spatial and molecular profiling technology that generates digital whole transcriptomes and profiling data for validated protein analytes from tissue (GeoMx® Digital Spatial Profiler platform; NanoString Technologies, Inc.). Slides were first stained with fluorescently-labeled antibodies against CD3E, CD68, and GFAP and with DAPI to mark nuclei. We then selected regions of interest in both inflamed tissue (marked by dense immune cell infiltrate in the anterior horn) or control tissue (contralateral anterior horn areas with few immune cells present and posterior spinal cord areas). The immuno-oncology probe library (NanoString; 1,793 genes plus 32 control genes, with an average of 5 probes per gene) was hybridized to the spinal cord section. Ultraviolet light was then focused on the regions of interest to cleave linked DNA oligonucleotides with unique molecular identifying sequences to each probe. The cleaved oligonucleotides were then sequenced and quantified using next generation sequencing (Illumina). Reads were normalized either to the third quartile of reads in each region of interest (NanoString proprietary software) or by a fit of normal distributions using the ashr package[13] in R software (v. 3.6.3). We then compared the type and number of gene transcripts detected in inflamed versus control tissues. To determine which biological pathways were upregulated, gene transcripts with statistically significant upregulation in inflamed tissue were entered into the Gene Ontology (GO) knowledgebase (geneontology.org). We analyzed results from the GO biological process complete dataset. Both

raw transcript data and normalized data are available for download or interactive searching and visualization through a web-based interface (Shiny application, RStudio) at url http://vogtviruslab.med.unc.edu/evd68_humanspinalcord/.

STATISTICAL ANALYSIS

Principal component analysis (PCA) comparing immunomes of regions of interest was performed with variance stabilizing transformation using DESeq2 package in R. We generated volcano plots using the EnhancedVolcano package and used the ashr package in R to provide empirical Bayes shrinkage estimators for effect sizes. Gene ontology analysis used the Fisher's Exact test with correction by calculation of false discovery rate.

RESULTS

VIRUS DETECTION

We used an amplified *in situ* hybridization (ISH) technique to visualize EV-D68 genomic RNA in lung and spinal cord sections. EV-D68 RNA was almost absent from the lung at this time point; we found only very rare cells with the appearance of one or two genomes of EV-D68. If this patient had lung infection, this site of infection appeared to have largely resolved, which is consistent with the timing of clinical resolution of prodromal fever and/or respiratory symptoms near the onset of paralysis that is seen in most cases of AFM. In two different segments of spinal cord, we noted occasional EV-D68 RNA-containing neurons in one section and abundant RNA-containing neurons in another, cervical section (Figs. 1A, S1A), correlating with his upper limb weakness. RNA was present in both the cell bodies and the axons. RNA was not clearly found in any glial cells or other non-neuronal cell types. Immunohistochemistry (IHC) staining for the

neuron-specific marker NeuN revealed that cells with with EV-D68 RNA stained positive for NeuN in serial sections with only rare exception (Fig. S2). IHC staining for the EV-D68 VP2 capsid protein in serial sections of spinal cord revealed viral protein was present in the same cells and cell structures in which viral RNA was detected (Figs. 1B, S1B).

IMMUNE STAINING

Using IHC, we characterized the inflammatory infiltrate present in the infected spinal cord segment. The most predominant immune cells detected were macrophages (Fig. S3A). Lymphocytes were also present, and these were chiefly T cells, with rare B cells detected (Fig. S3B), similar to what was previously reported[11]. Of those T cells present, nearly all were CD8+ cytotoxic T cells and very few were CD4+ helper T cells (Fig. S3C).

SPATIAL IMMUNE TRANSCRIPTOMICS

Using an established panel of labeled probes that focused on 1,793 genes related to immunology and oncology, we compared the expression of these genes' transcripts in inflamed areas of the spinal cord versus control, non-inflamed areas. PCA confirmed that the transcripts from the visibly inflamed areas clustered together separately from the control areas (Fig. S4A). 58 genes were significantly upregulated in the inflamed tissues (Fig. S4B). Notably, analysis of transcripts using NanoString software identified 51 significantly upregulated genes, with 33 genes identified by both NanoString and the alternate R software-based analytic method. These upregulated genes are factors in many biological processes, but the most frequently identified upregulated biological pathways were involved in antigen processing for presentation on MHC-I molecules, consistent with the presence of a CD8 T cell infiltrate seen in IHC (Fig. S3C).

DISCUSSION

By identifying a unique case that occurred prior to widespread recognition of AFM and studying autopsy specimens, we better understand the pathogenesis of an emerging public health threat. While the main limitation of this study is its nature as a single case report capturing a single timepoint in disease, likely few autopsy studies will be possible in future due to increased awareness in the pediatric provider community and the effectiveness of modern supportive critical care when a case of AFM is now identified.

Regarding pathogenesis, this study reveals that EV-D68 directly infects spinal cord neurons and that a corresponding robust immune response is present. Either cytopathic effect from infection or tissue destruction of dysfunctional inflammation, or likely both factors, could contribute to death of motor neurons causing weakness. The composition of the inflammatory infiltrate, cytolytic CD8+ T cells and phagocytic CD68+ macrophages, plus prior staining showing perforin in the neurons[11] further lends plausibility to the role of immunopathogenesis contributing to AFM. Therefore, optimum acute treatment of AFM likely requires a multi-pronged approach focused on antiviral and anti-inflammatory strategies. Given the rarity of AFM, with 668 confirmed cases in the United States since 2014, designing a study with the power to determine efficacy of any therapeutic is challenging, making informed choices based on pathogenesis important. We observed evidence of viral replication in neurons days after onset of weakness, so direct antiviral therapies like monoclonal antibodies[14] or small molecule antiviral drugs might be of benefit at that point in infection. Further, anti-inflammatory medication may diminish immunopathogenesis, although balancing immune suppression with ongoing viral replication requires careful consideration. Intravenous immune globulin (IVIG) from all

manufacturers tested contained EV-D68 neutralizing antibodies[15], and IVIG has anti-inflammatory action, so this treatment may be preferred until more specific antiviral and anti-inflammatory drugs are developed and evaluated.

This study also serves to compare natural EV-D68 infection to existing laboratory models. EV-D68 tropism at this acute timepoint in this patient was largely restricted to neurons, as nearly all infected cells also stained for NeuN. In some paralytic murine models of infection, EV-D68 also was largely restricted to neurons in the spinal cord[7,8], lending validation to these features of those animal experiments as models of AFM. We highlighted the rare exception of a cell staining for EV-D68 RNA but not apparently staining for NeuN, which could represent an infected glial cell. Alternatively, this finding may represent a glial cell that phagocytosed infected cellular debris. While iPSC-derived neurons in culture can be infected by EV-D68[9,10], iPSC-derived astrocytes also were infected by EV-D68[10], which is incongruent with all but this rare observation. Due to technical limitations, we could not co-stain with GFAP or any other marker of astrocytes. Also, this study represents a single case and a single time point in infection. Therefore, this study does not exclude the possibility that EV-D68 could infect astrocytes or other non-neuronal cell types.

We present the transcriptomic data gathered here primarily for hypothesis generation for further studies, as many limitations are inherent to this analysis. We were unable to study the whole transcriptome. Including control regions of interest from posterior spinal cord may not be the best comparison, but we were unable to use completely uninflamed sections of anterior spinal cord to select control regions of interest. Nonetheless, the data could prove valuable for study given the rarity of this sample. For example, some investigators are profiling the transcriptomes of cells in the cerebrospinal fluid of patients with AFM, so this data set from spinal cord tissue

serves for relevant comparison. The ontology of the upregulated pathways is consistent with the immune infiltrates seen, as we would expect both infected cells and macrophages to upregulate MHC class I presentation and CD8+ T cells to respond to this stimulation.

Aside from its nature as a study of a single individual, other caveats are worth noting regarding this case. The detection of any virus in cerebrospinal fluid of AFM patients is rare[6], yet this patient had EV-D68 detected in cerebrospinal fluid by RT-PCR[11]. This isolate from 2008 groups into clade C, yet most isolates detected since 2014 come from clades B and D[16], and it is possible B and D clade isolate pathogenesis could differ from that of clade C viruses in humans. However, the murine models that exhibit similar tropism as seen in this human infection use clade B viruses[7,8], so clade B viruses are capable of tropism in other mammals similar to what we observed with clade C virus.

Overall, these studies provide further evidence that EV-D68 infection of the spinal cord is a direct cause of AFM, now with insight into the pathogenesis of this process in humans, which may be due to a combination of direct effects of viral infection and resultant inflammation. This model is consistent with the presence of signal change in the anterior horn of the spinal cord in images obtained with magnetic resonance imaging of humans with AFM[17-19], and with many laboratory models of EV-D68-associated AFM[7-9]. Information derived from this case report may inform treatment approaches and further direction of laboratory studies. The study also validates the high value of conducting autopsies and biobanking tissues for cases of poorly explained infectious syndromes.

FIGURES

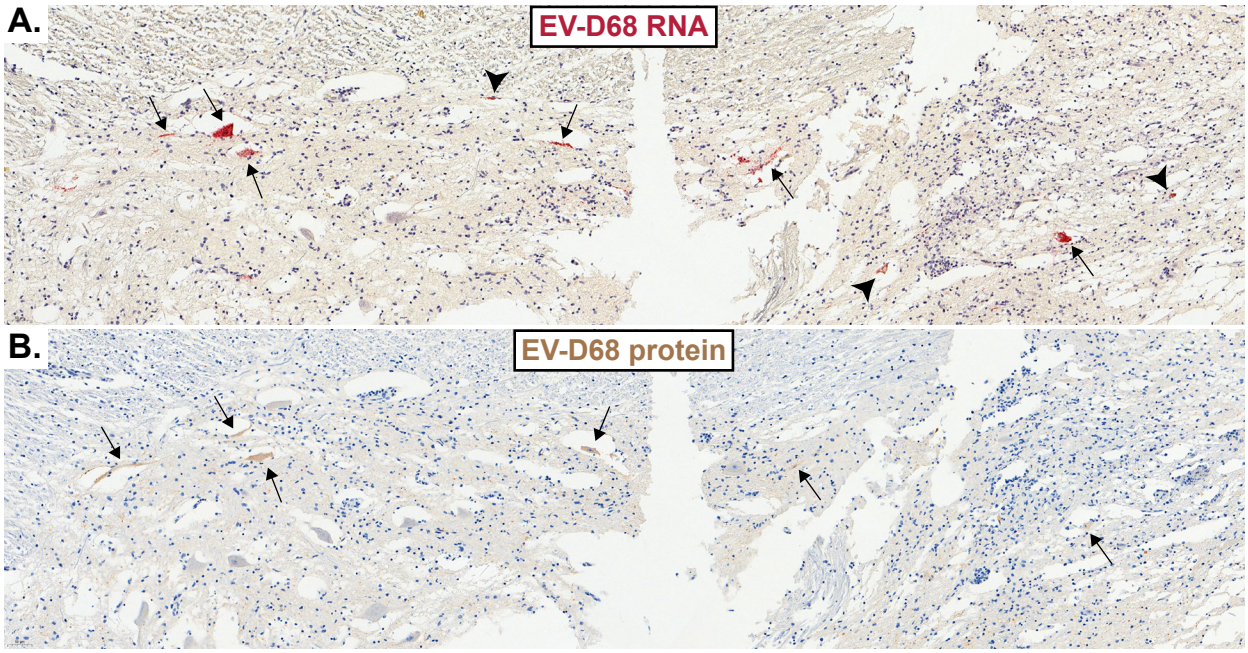

Figure S1. EV-D68 RNA and capsid protein are present in spinal cord anterior horn neurons.

In situ hybridization (A) or immunohistochemistry (B) demonstrate EV-D68-specific genomic RNA or viral capsid protein, respectively. In these serial sections of spinal cord, examples of neuronal structures staining for both RNA and protein are highlighted by arrows, whereas neuronal structures staing for RNA without a clear corresponding protein staining structure are highlighted by arrowheads. Neurons shown in Fig. 1 are also seen in these lower magnification images of the same sections.

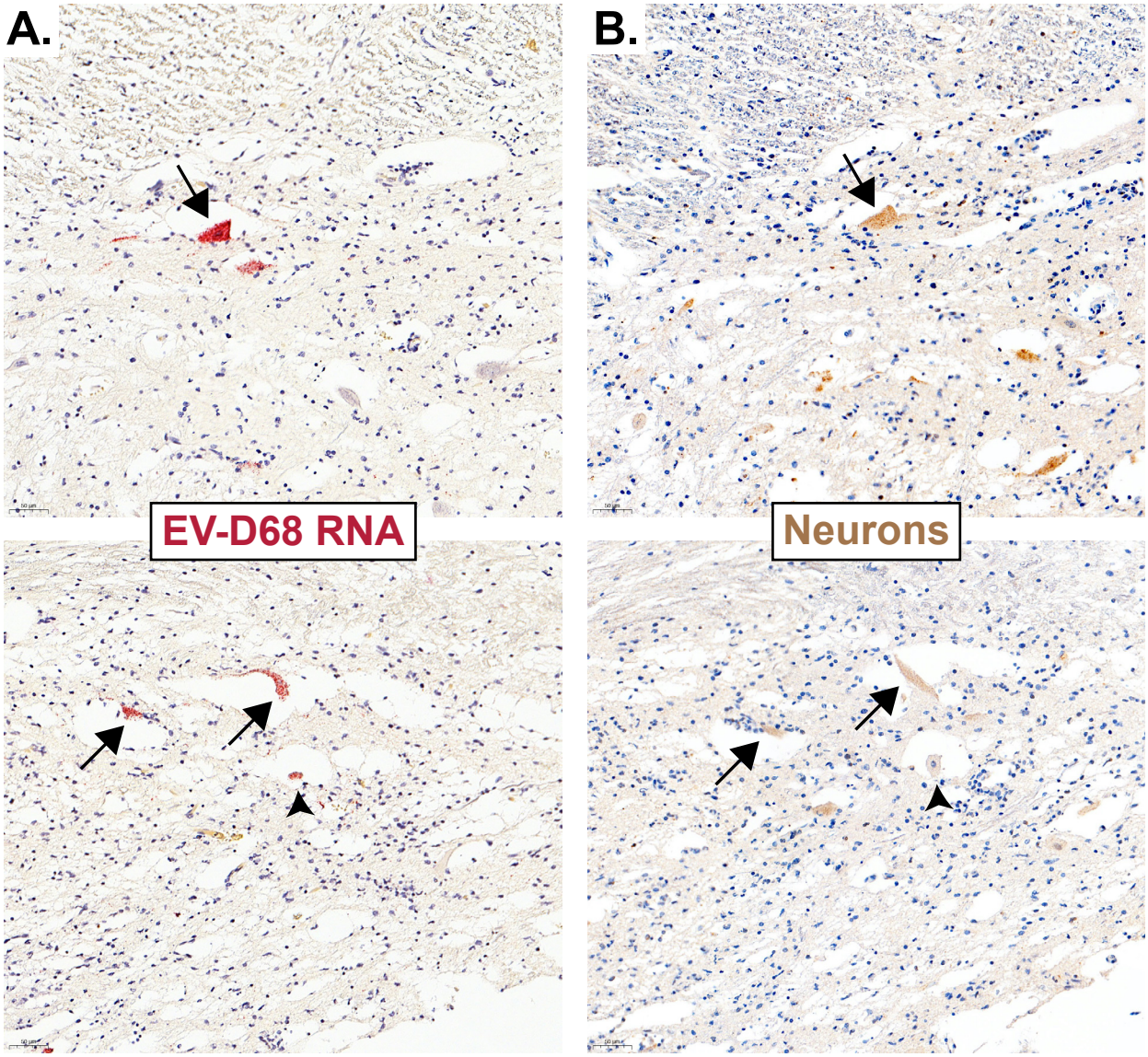

Figure S2. Most cells staining for EV-D68 RNA stain for neuron-specific marker NeuN. *In situ* hybridization (A) or immunohistochemistry (B) demonstrate EV-D68-specific genomic RNA or NeuN, respectively. NeuN is a specific marker of neurons. In these side-by-side serial sections of spinal cord, examples of neuronal structures staining for both EV-D68 RNA and NeuN are highlighted by arrows. A rare example of a cell staining for RNA but not for NeuN is highlighted by an arrowhead in the lower panels.

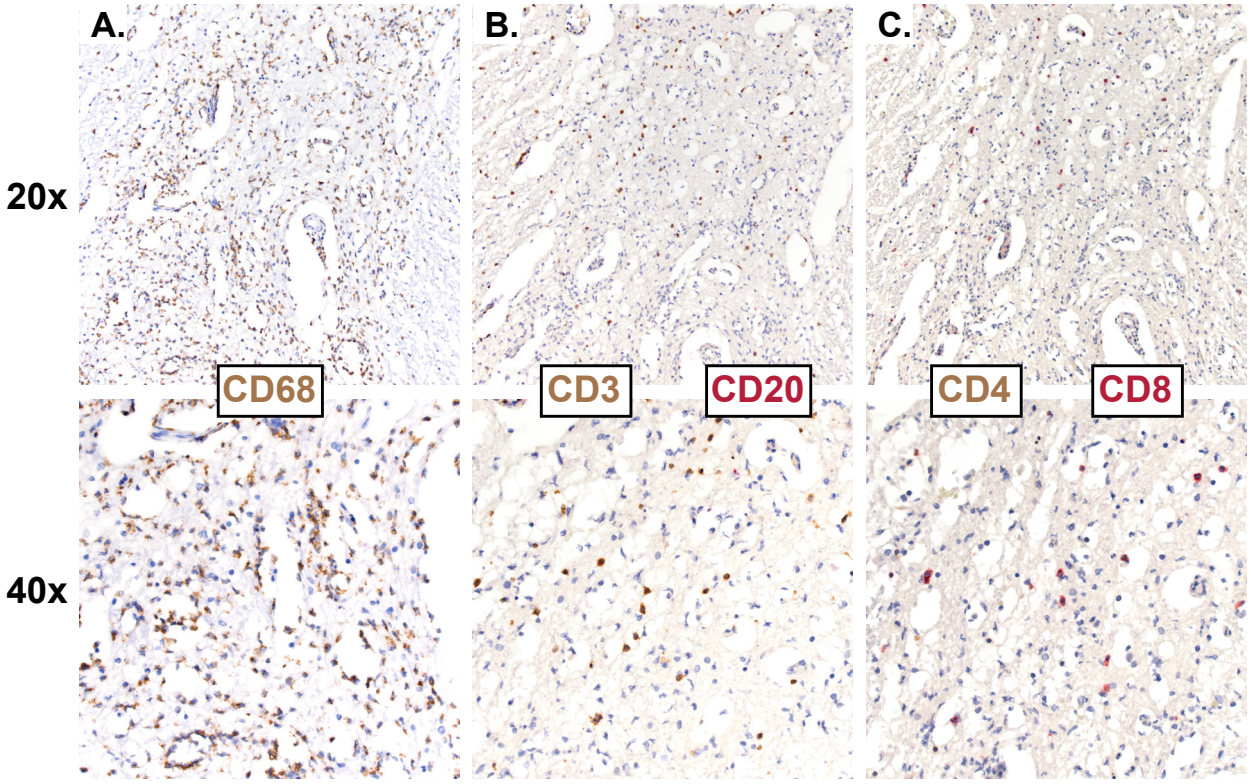

Figure S3. Macrophages and CD8+ T cells predominate in the inflammatory infiltrate of the EV-D68-infected spinal cord.

(A) Staining for CD68 reveals an infiltrate of predominantly macrophages. (B) Two-color IHC with co-staining for CD20 (red) and CD3 (brown) show few B cells but numerous T cells. (C) Co-staining for CD4 (brown) and CD8 (red) show that the T cells are predominantly cytotoxic T cells.

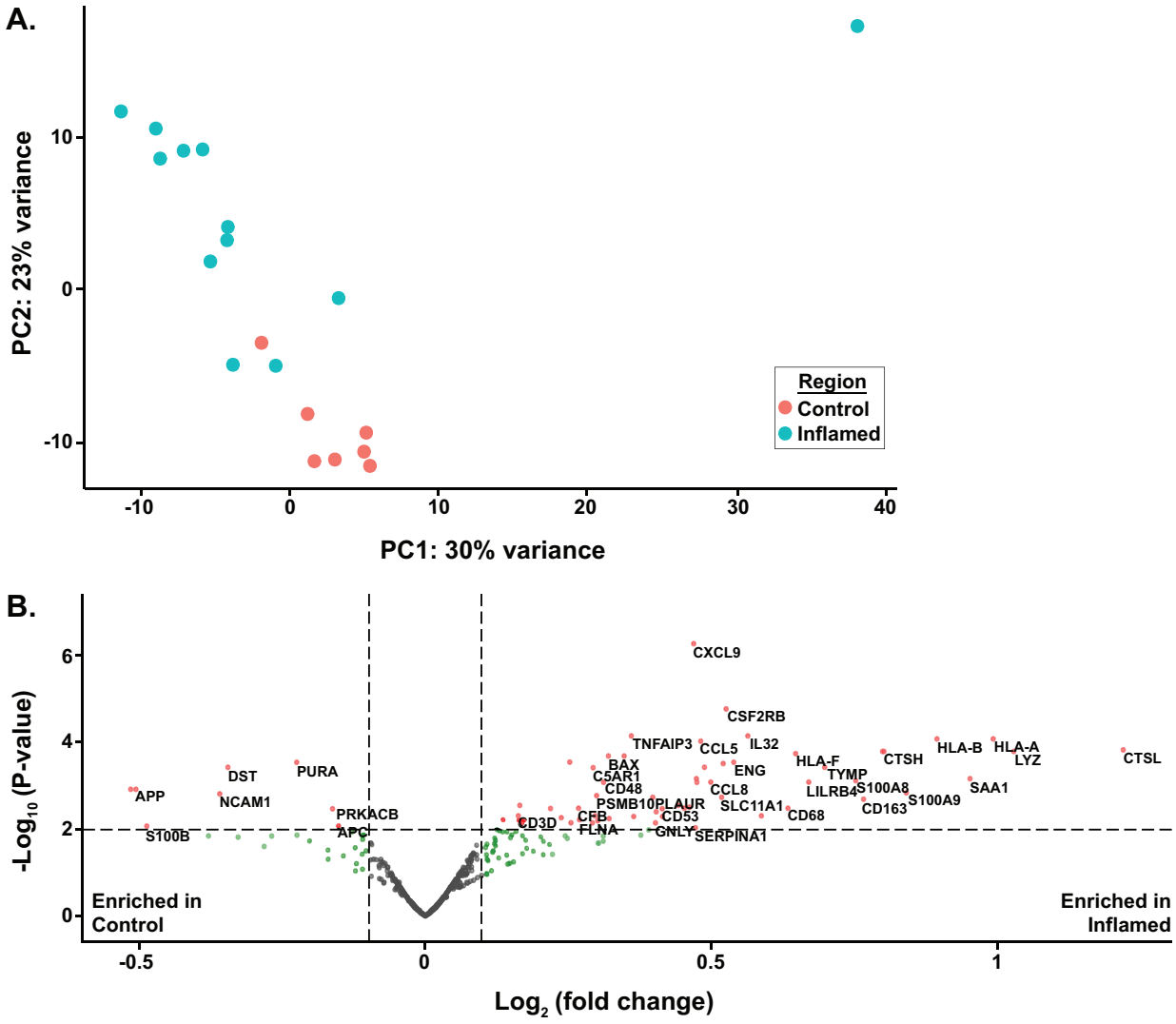

241

242 **Figure S4. Immune-related transcripts related to antigen presentation on MHC are**

243 **upregulated in EV-D68-infected spinal cord.**

244 (A) Principal component analysis of immune transcriptomes of twelve inflamed and seven

245 control regions of interest in the patient's spinal cord. (B) Volcano plot with each dot

246 representing an individual gene transcript. Transcripts upregulated in inflamed areas lie to the

247 right and those with lower P values lie higher on the graph.

248

ACKNOWLEDGMENTS

We acknowledge assistance from the Vanderbilt Translational Pathology Shared Resource supported by NCI/NIH Cancer Center Support Grant 5P30 CA68485-19 and the Shared Instrumentation Grant S10 OD023475-01A1 for the Leica Bond RX. We acknowledge assistance from the Bioinformatics and Analytics Research Collaborative, which is supported by University of North Carolina at Chapel Hill School of Medicine strategic funds. W.A. Nix and M.S. Oberste at the Centers for Disease Control and Prevention identified the patient's EV-D68 sequence and clade designation. Dr. Vogt was supported by grant K08 AI153125 from the National Institute of Allergy and Infectious Diseases and the Pediatric Infectious Diseases Society-St. Jude Children's Hospital Fellowship Program in Basic Research. The Fellowship was funded by St. Jude Children's Research Hospital and jointly sponsored by the Pediatric Infectious Diseases Society and St. Jude Children's Research Hospital. Dr. Crowe was supported by grant U19 AI117905 from the National Institute of Allergy and Infectious Diseases.

REFERENCES

1. Sejvar JJ, Lopez AS, Cortese MM, et al. Acute flaccid myelitis in the United States, August-December 2014: results of nationwide surveillance. Clin Infect Dis 2016;63:737-45.

2. Van Haren K, Ayscue P, Waubant E, et al. Acute flaccid myelitis of unknown etiology in California, 2012-2015. JAMA 2015;314:2663-71.

3. Messacar K, Schreiner TL, Maloney JA, et al. A cluster of acute flaccid paralysis and cranial nerve dysfunction temporally associated with an outbreak of enterovirus D68 in children in Colorado, USA. Lancet 2015;385:1662-71.

4. Murphy OC, Messacar K, Benson L, et al. Acute flaccid myelitis: cause, diagnosis, and management. Lancet 2021;397:334-46.

5. Centers for Disease Control and Prevention. Acute Flaccid Myelitis Frequently Asked Questions. (Accessed September 23, 2021, at https://www.cdc.gov/acute-flaccid-myelitis/faqs.html.)

6. Messacar K, Asturias EJ, Hixon AM, et al. Enterovirus D68 and acute flaccid myelitis-evaluating the evidence for causality. Lancet Infect Dis 2018;18:e239-e47.

7. Hixon AM, Yu G, Leser JS, et al. A mouse model of paralytic myelitis caused by enterovirus D68. PLoS Pathog 2017;13:e1006199.

8. Morrey JD, Wang H, Hurst BL, et al. Causation of acute flaccid paralysis by myelitis and myositis in enterovirus-D68 infected mice deficient in interferon alphabeta/gamma receptor deficient mice. Viruses 2018;10.

9. Hixon AM, Clarke P, Tyler KL. Contemporary circulating enterovirus D68 strains infect and undergo retrograde axonal transport in spinal motor neurons independent of sialic acid. J Virol 2019;93.

10. Rosenfeld AB, Warren AL, Racaniello VR. Neurotropism of enterovirus D68 isolates is independent of sialic acid and is not a recently acquired phenotype. mBio 2019;10.

11. Kreuter JD, Barnes A, McCarthy JE, et al. A fatal central nervous system enterovirus 68 infection. Arch Pathol Lab Med 2011;135:793-6.

12. Knoester M, Helfferich J, Poelman R, et al. Twenty-nine Cases of Enterovirus-D68-associated Acute Flaccid Myelitis in Europe 2016: A Case Series and Epidemiologic Overview. Pediatr Infect Dis J 2019;38:16-21.

13. Stephens M. False discovery rates: a new deal. Biostatistics 2017;18:275-94.

14. Vogt MR, Fu J, Kose N, et al. Human antibodies neutralize enterovirus D68 and protect against infection and paralytic disease. Sci Immunol 2020;5.

15. Zhang Y, Moore DD, Nix WA, Oberste MS, Weldon WC. Neutralization of Enterovirus D68 isolated from the 2014 US outbreak by commercial intravenous immune globulin products. J Clin Virol 2015;69:172-5.

16. Midgley SE, Benschop K, Dyrdak R, et al. Co-circulation of multiple enterovirus D68 subclades, including a novel B3 cluster, across Europe in a season of expected low prevalence, 2019/20. Euro Surveill 2020;25.

17. Maloney JA, Mirsky DM, Messacar K, Dominguez SR, Schreiner T, Stence NV. MRI findings in children with acute flaccid paralysis and cranial nerve dysfunction occurring during the 2014 enterovirus D68 outbreak. AJNR Am J Neuroradiol 2015;36:245-50.

18. Gordon-Lipkin E, Munoz LS, Klein JL, Dean J, Izbudak I, Pardo CA. Comparative quantitative clinical, neuroimaging, and functional profiles in children with acute flaccid myelitis at acute and convalescent stages of disease. Dev Med Child Neurol 2019;61:366-75.

19. Okumura A, Mori H, Fee Chong P, et al. Serial MRI findings of acute flaccid myelitis during an outbreak of enterovirus D68 infection in Japan. Brain Dev 2019;41:443-51.